Design and Deployment methods for a Martian exploration airship

Philippe MACHERET *† *and Guillaume DEL PEDRO**
* *Ecole Polytechnique Federale de Lausanne*
Route Cantonale, 1015 Lausanne, Switzerland
philippe.macheret@epfl.ch · guillaume.delpedro@epfl.ch
†Corresponding author

Abstract

This feasibility study focuses on the development of a Martian airship, seeking to ensure a secure unfolding process within the harsh Martian environment. Four distinct methods are explored for the unfolding and inflation phase, aiming to guarantee a safe deployment. The study also presents solutions involving two bonded layers: one preserving hydrogen and the other resisting mechanical stresses on the envelope. Hydrogen storage and transportation are addressed as well as the attachment system of the envelope to the gondola, paving the way for future Martian exploration.

1. Introduction

Exploring Mars has traditionally relied on orbital satellite observations and ground-level investigations using rovers. However, there remain fascinating yet inaccessible areas such as craters and cliffs that pose challenges to exploration with the current means. To overcome this limitation, the concept of an exploration airship has emerged, capable of navigating the steepest Martian terrain equipped with advanced scientific instruments such as cameras, spectrometers, and hyperspectral cameras. A preliminary feasibility study on employing such airships for exploring the slopes of Valles Marineris was presented at GLEX 2021 [1], followed by subsequent work at IAC 2022 [2].

Designing a lighter-than-air vehicle for the thin and cold Martian atmosphere presents a significant challenge. While NASA's successful deployment of the Ingenuity helicopter demonstrated the potential for powered flight on Mars, its limited flight duration and the need for frequent recharging restrict its exploration capabilities. This study proposes a lighter-than-air exploration balloon equipped with scientific instruments. Such airships have been used in planetary exploration, as demonstrated by the Soviet Union's Vega missions to Venus in the 1980s. Later, various space agencies, including NASA's Mars Aerobot Balloon Study (MABS) and CNES's Montgolfière Infra-Rouge (MIR), explored and developed concepts for exploration balloons. Additionally, recent advancements in powered aerostatic flight on Earth, exemplified by the Stratobus concept from Thales, have renewed interest in long-term exploration missions.

1.1 Study History and current airship overview

The feasibility study of a Martian airship began in 2020 with the collaboration of WoMars association, eSpace, and the Mars Society Switzerland, initiated by Romeo Tonasso. The project's first phase, presented at GLEX 2021 [1], was followed by a second round of feasibility studies in 2021, which aimed to refine models, validate hypotheses, and initiate the design iterations of selected subsystems. These advancements were presented at IAC 2022 [2].

To understand the study, it is essential to have a look at the airship's current configuration. The airship is projected to have a total mass of 950 kg, with a payload capacity of 10 kg allocated for a hyperspectral camera, data storage and communication. Contingencies have been incorporated, considering the significant uncertainty in several subsystems. The envelope, weighing approximately 400 kg, is made of thin layers of Mylar and Dyneema. The operation zone is Valles Marineris. With its higher atmospheric density, it holds particular promise for the airship's performance. The increased lift due to the denser atmosphere coupled with the valley's depth offering an extended descent path for aerobraking presents an ideal terrain for long-term exploration. The current design features a 43 m diameter envelope filled with hydrogen as the lifting gas. Propulsion is achieved through propeller sets mounted on deployable arms attached to the gondola, which remains stowed during the journey to Mars. A battery system is essential to provide continuous power, even during night-time operations. Considering a conservative energy density of 160 Wh/kg, a

battery mass of 130 kg is required to ensure the airship's survival throughout the night, although recent advancements in energy density may reduce this mass. Energy generation is ensured by solar cells, which serve to recharge the batteries during the day while powering other subsystems.

This study continues the previous work and addresses crucial aspects including the evaluation of deployment strategies for atmospheric entry, descent, and landing (EDL), hydrogen storage, as well as the envelope composition and stress analysis.

2. Deployment methods

In this part of the study, the crucial task of safely deploying and inflating the envelope in an unmanned manner is discussed. The Martian atmosphere poses a challenge, being too thin to provide adequate deceleration while simultaneously generating aerodynamic heating. For missions carrying heavy payloads on Mars, a robust parachute with a large diameter or even a propulsion system becomes essential. Ground-level winds generally remain below 20 m/s, but at higher altitudes, they can exceed 120 m/s, potentially altering the landing craft's trajectory. Consequently, the EDL process becomes intricate for missions involving substantial payloads, yet not insurmountable. Notably, the Mars 2020 Mission achieved a successful landing through the Skycrane [3]. In the next sections, four distinct options are explored, considering their applicability and effectiveness.

2.1 Orbit Deployment

2.1.1 Concept

The first concept is a deployment in orbit. This solution is considered by the Mars Society Deutschland for their balloon Archimedes [4]. This solution allows a slow deployment and a slow inflation in an environment with fewer constraints. The aim is to avoid the potential issues encountered during inflation from the ground or during the descent phase. All those factors do not exist in space. Inflatable structures in space are not a new idea: Hypersonic Inflatable Aerodynamic Decelerators (HIAD) are an example [5].

The concept of operations, see figure 1, is the following. When the spacecraft is in Mars orbit, the airship is unfolded and the inflation starts (1) (the (#) corresponds to the number on the concept drawing). This operation is performed with little time constraints. When the envelope is fully inflated, the spacecraft is detached. Then, the airship starts its fall to Mars (2). The gondola and the envelope are protected by a removable thermal shield layer. The balloon enters the thin atmosphere and decelerates to subsonic speed. When it has reached a sufficient altitude, the thermal protection layer is released (3). Finally, the airship can deploy its propulsion system and starts navigating (4). To stop its fall, the airship uses drag force and buoyancy force. The buoyancy is critical to totally stop the fall and start the flying phase. This last deceleration can only occur when the Martian air is dense enough. A very deep, lower than -3km MOLA (Mars Orbiter Laser Altimeter), and large "landing zone" must be targeted in Valles Marineris to guarantee the success of this solution.

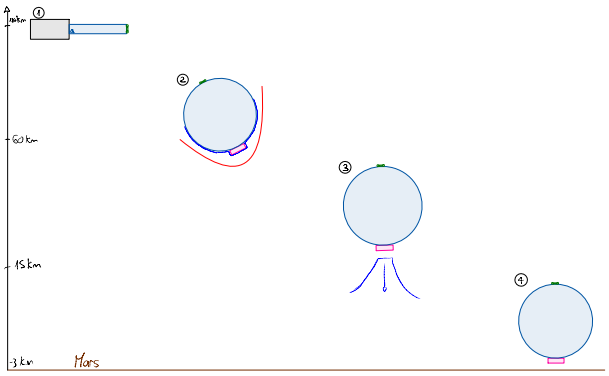

Figure 1: Orbital inflation concept

2.1.2 Thermal protection

The main considerations for this solution are thermal load and dynamic pressure. Selecting a thermal protection system (TPS) is not a straightforward task. The conventional rigid heat shield, typically used on landing craft, is ruled out due

to the size of the inflated balloon. Although a HIAD is a better choice, it is suboptimal in this case because the airship already creates a large resistant area. It is not suitable for this application, and its mass would be significant. Instead, an additional layer of flexible thermal protection added at the interface of the balloon is preferred. This layer can be dropped to reduce the airship's weight at the desired altitude. Two possibilities for the TPS are passive TPS and ablative TPS. Due to the low heat flux involved (see Table 3), a passive TPS is chosen. The objective is to determine the temperature rise inside the balloon caused by conduction, as there is contact between the TPS and the envelope. The temperature difference affects the pressure and mechanical properties of the envelope. The temperature tolerance of Mylar is low, around 415 K. In terms of structural stress, the resulting pressure is lower than atmospheric pressure at ground level.

A 3-layer design is selected for the flexible TPS, as shown in Table 1. Nextel 312 is chosen for its radiative capacity, low conductivity, high yield, and low density. Silica aerogel is selected for its excellent insulation performance and very low density. This insulation layer protects the balloon against thermal conduction generated by the high temperature of Nextel. The aluminum layer is the final layer and aims to shield the envelope from radiation emitted by Nextel. Since the aerogel layer is highly transparent, the aluminum layer reflects the radiation in the opposite direction of the airship. The minimum thickness of aerogel required is 15 mm to ensure the Mylar layer stays below its temperature limit (see figure 2), as it is the most restrictive constraint. Due to the large surface area to cover, the estimated mass of the TPS is 4.095 tons, which is 4.39 times the mass of the airship.

Table 1: TPS layers

Material	thickness [mm]	areal density [g/m^2]
Nextel 312	0.33	326
Silica aerogel	15	825
Aluminum	0.015	0.405
Total	15.345	1151.405

A second prototype of the TPS involves introducing holes in the aerogel layer. With a 50% emptied hexagonal pattern, the quantity of aerogel is reduced by 2 and the TPS mass by 1.5 compared to the initial design. The thermal protection is still ensured since there are voids in the aerogel holes. However, the pressure on the surface changes. A numerical simulation of the stress on the flexible envelope with the emptied hexagonal pattern is needed to validate this design. By performing a heat flux balance at the external wall of the heat shield, the temperature of the TPS can be computed.

To get thermal results, initial conditions are needed to make a cinematic simulation. The choice of the angle of entry is a trade-off between:

- High peak temperature and high heat flux, but low thermal load for high angle
- Low peak temperature, low heat flux, but high thermal load for low angle

The temperature evolution until the peak is shown on the figure below and the different maximums happen at an altitude of 40 to 60 km MOLA.

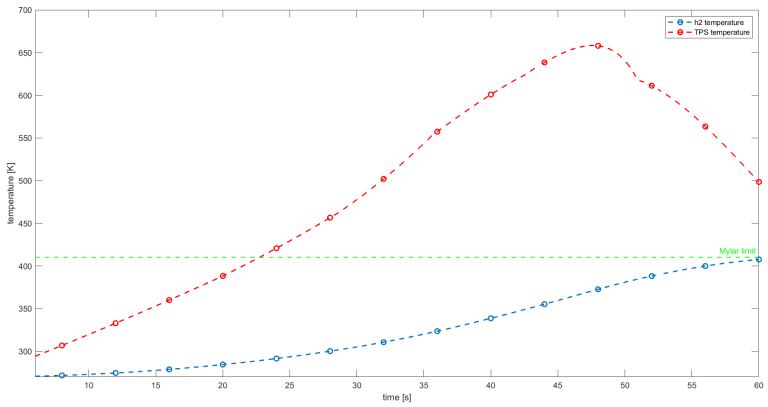

Figure 2: Temperature simulation

Table 2: Initial conditions

Altitude	120 km
Flight angle	-14 °
Speed	5 km/s
Resistant area	1661.9 m^2
Entry mass	4900.4 kg

Table 3: Maximum values

Maximum	Value	Time [s]	Altitude [km]
Earth g-charge [g]	16.69	56	50.58
$\dot{q}_{\text{conv}}$ $[W/m^2]$	7676.1	48.7	58.21
$\dot{q}_r$ $[W/m^2]$	1989.7	47	60.24
T_w max [K]	658.29	47.6	59.52
T_b max [K]	411.01	65.1	44.06
Dynamic pressure [Pa]	493.65	56	50.57
Heat load $[j/m^2]$	$2.35 \cdot 10^5$	-	-
Total heat $[j]$	$3.91 \cdot 10^8$	-	-

2.2 Mid Air Deployment

The second option is Mid Air Deployment, as illustrated in Figure 3. The concept of this deployment solution is to take advantage of the descent phase to deploy and inflate the envelope. This approach was experimented by the Jet Propulsion Laboratory (JPL) for their balloon in Earth's upper atmosphere [6]. During the atmospheric descent (1), the balloon is deployed through parachute release, and inflation occurs during the fall (2-4). The buoyancy generated allows the airship to stop its descent before reaching the ground (5). However, this solution requires a landing craft for entry into the atmosphere. The primary consideration is whether the heavy airship can stop its fall before making contact with the ground. Consequently, the inflation process must be fast enough to enable the separation of the balloon and the reduction of its mass. Otherwise, the descent of the balloon will be uncontrolled.

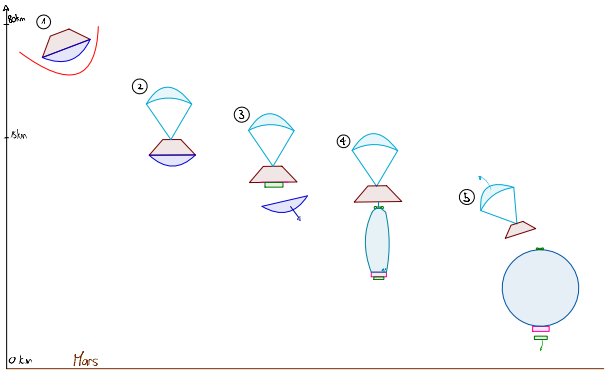

Figure 3: Mid Air Inflation Concept

To determine the maximum inflation time $t_{\max}$, a descent simulation is conducted with a total initial mass of $M = 2300$ kg. At the end of the inflation, when the hydrogen tank is dropped and the parachute is released, the mass decreases to $M = 930$ kg. In this configuration, the calculated $t_{\max}$ is 290 seconds. This short time frame makes this deployment solution very difficult. Several issues arise with this inflation speed. The release of hydrogen must occur at a rate greater than 100 g/s, which requires a rapid hydrogen release mechanism that also affects the storage system. Moreover, there are concerns about the fluid temperature at such high speeds, in addition to the risk of shock. However, the main problem associated with this deployment technique is the potential for envelope tearing. The interaction between the atmospheric flow and the structure of the airship generates vibrations that can lead to the envelope destruction. JPL encountered this problem with a large balloon (diameter > 12 m) during their experiments. Considering the current diameter of the airship is approximately 43 m, the stress on the structure will be even higher and will persist for a longer duration. Furthermore, JPL's experiments were conducted at low dynamic pressure (around 5 Pa), whereas this deployment strategy will encounter a peak dynamic pressure of approximately 31 Pa according to the simulation.

2.3 Powered Mid Air Deployment

The third concept is Powered Mid Air Deployment, which serves as a solution to address the challenges encountered in the previous deployment method. This concept draws inspiration from the Mars 2020 Mission's landing technique, where a Skycrane was used to safely land the rover [3]. In this situation involving a high descent speed, a propulsion system can be installed beneath the spacecraft to decelerate the descent and allow additional time for inflation (4). The propulsion system is initiated at a specific speed and altitude to ensure a controlled deceleration (5). As the envelope unfolds in the air, the propulsion system remains active until inflation is complete. Subsequently, the propulsion system and hydrogen tank are detached, allowing the balloon to start its flight (6). The concept is shown below.

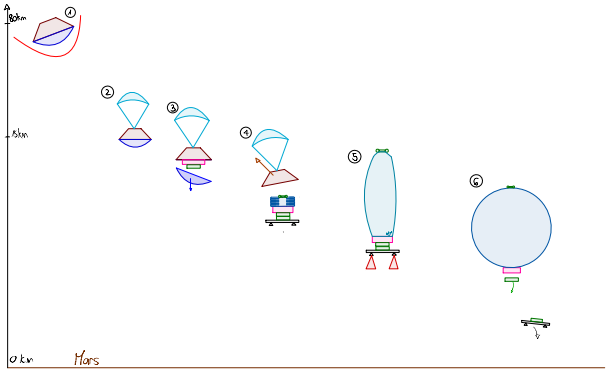

Figure 4: Powered Mid Air inflation concept

The parameters for this solution depend on the results of the analysis conducted on the Mid Air deployment, particularly the inflation time, landing craft speed, and mass. However, a significant amount of propellant (over 1.7 tons) is required only to achieve a $\Delta V = 25 m/s$ during $t_{\max}$. Consequently, to extend the inflation time, additional propellant will be needed, further increasing the overall mass. As a result, this solution exhibits inefficiency. Additionally, this method increases the complexity compared to the previous one. Even at low speeds, there remains a risk of envelope destruction due to vibrations. Nonetheless, the Powered Mid Air concept offers the potential to guide the airship toward a precise landing location.

2.4 Ground Deployment

The fourth option involves deploying the airship after landing on the Martian soil. The concept is illustrated in figure 5. The landing craft uses propulsion to control its descent and safely lands on the surface (1-6). Following this, the airship unfolds and initiates the inflation process. Once fully inflated, the balloon begins flying while the landing craft remains on the ground (7). This deployment solution allows for a slow and controlled inflation process on the Martian surface, free from speed or heat constraints, and with minimal stress on the airship's structure. However, despite these advantages, there are still potential risks and challenges associated with the unfolding and inflation phase.

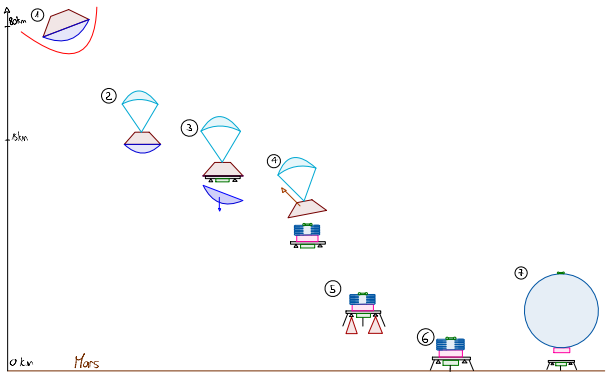

Figure 5: Ground inflation Concept

2.4.1 Inflation phase

The unfolding and inflation phase is critical to the overall success of the mission. Unlike the other deployment methods, which encounter fewer external hazards during this step, there is a risk of damaging the envelope during ground inflation. During the inflation phase, the envelope is susceptible to hit its immediate surroundings due to wind. To ensure a safe release, sensors are incorporated into the landing craft, and an appropriate moment is selected to initiate this phase. However, even with careful timing, there is a possibility that wind may push the balloon downwards, causing the envelope to touch the ground and potentially sustain damage.

The unmanned inflation of the airship is the most dangerous phase of this deployment method, requiring a packing technique that avoids unwanted contact with the Martian surface or the surrounding spacecraft structure. Consequently, a packing technique is implemented to safely unfold the balloon during the inflation process, ensuring precise control based on the amount of lifting gas being filled in. A major challenge comes with PV on top of the envelope, which adds more weight to the system.

The considered folding pattern is the "inverted-cone" technique [7]. While being originally developed for airbags, this folding technique proves applicable to the airship due to the shared requirement of compact packing and reproducible and predictable expansion. One challenge is that the airship cannot fly until it reaches a certain volume. Various auxiliary systems have been considered to support the envelope during inflation. The first option involves an auxiliary balloon that extracts and unfolds the main balloon from its hull. However, this approach is very suboptimal as it increases the overall mission mass and requires a large auxiliary balloon, which, in turn, necessitates its own auxiliary balloon. The second option involves using an inflatable supporting cone to guide the upward inflation of the balloon [8]. Before achieving buoyancy, the envelope glides on the smooth surface of the supporting cone, facilitating its safe unfolding. The diameter of the cone must be large enough to prevent the envelope from overflowing on the sides during inflation. The Martian atmosphere can provide the gas to fill the cone.

2.5 Comparative Summary

The following table presents a quantitative comparison of the different solutions, providing a score from 0 (worst) to 10 (best) for each parameter:

		Score out of 10			
Criteria	weighting factor	Orbital	Mid Air	P-Mid Air	Ground
Mass system	1	3	8	4	8
Mission complexity	1	7	6	4	4
Risk	2	6	2	3	6
Structural Stress	1	5	2	3	9
Inflation condition	2	9	3	3	9
Unfolding mechanism	1	5	8	8	3
Thermal load	1	3	8	8	9
Propulsion & control	1	8	8	4	5
Total		6,10	5,00	4,30	6,80

Figure 6: Comparison score for deployment

From figure 6, The Ground deployment method is the best out of the 4. Even if it is the most complex and the unfolding phase presents a significant challenge, this solution offers safety, low stress, and slow inflation time. However, the unfolding mechanism needs further work and numerical simulation.

The Mid Air and Powered Mid Air deployment are interesting due to their simple unfolding phase. However, the unpredictability of the fall, along with factors such as shock propagation, trajectory modifications, the dynamic movement of the envelope leading to potential destruction, and the fast release of hydrogen make this solution unsafe. These uncertainties are further amplified by the large size of the envelope. Concerning the Powered Mid Air solution, it is highly suboptimal due to the significant amount of fuel required. The only advantage it offers is a reduction in fall speed without clearly solving the mentioned problems.

The Orbital deployment method is also a viable option, but it requires modifications to the envelope material, as Mylar is unable to withstand high temperatures. Another material would reduce the thickness of the TPS, resulting in a reduction of the mass of the whole system. However, this would mean changing the entire envelope and starting the project all over again.

3. Hydrogen storage

The chosen lifting gas is hydrogen and 33 kg of it is required to fill the envelope [9]. It has to be stored in safe conditions including during the flight to Mars, the EDL, and the inflation. After the inflation phase, the vessel and its auxiliary system are dropped from the airship to reduce the weight and to allow buoyancy. To compensate for hydrogen loss through the envelope and extend the airship's lifespan, an additional smaller hydrogen tank can be considered on the gondola.

The primary challenge lies in maximizing the quantity of hydrogen stored while minimizing the tank's mass. Hydrogen storage is complicated due to its low density, low condensation temperature, and high diffusion capacity. Several storage options exist, including liquid hydrogen, high-pressure hydrogen, low-pressure hydrogen, and metal hydride storage. However, the low-pressure storage option will not be discussed due to its significantly low density (approximately 0.090 kg/m^3).

3.1 Liquid hydrogen

Transporting a large quantity of hydrogen in the liquid state is the most mass-effective approach. Liquid hydrogen (LH2) offers a density of $71 kg/m^3$, resulting in an appealing weight ratio (mass of hydrogen / mass of vessel) of around 18%. However, this solution requires a complex storage vessel capable of maintaining the required temperature of $-253°C$. Additionally, a heat exchanger system is necessary to compensate for heat flux, which consumes energy. Boil-off is a significant concern, with a loss rate of approximately 0.5% per day. To compensate for this loss, the initial mass of hydrogen must be at least four times higher than the useful mass, making this option impractical for the mission's duration.

3.2 Compressed hydrogen

High-pressure storage of hydrogen (cH2) presents challenges mainly related to the tank's design. The tank must withstand pressure, external hazards, and have low permeability to avoid leaks. Commercial high-pressure tanks of up to 70 MPa are available [10]. The main advantage of compressed hydrogen storage is its simplicity and the speed at which hydrogen can be retrieved from the tank. The density is relatively high at $42 kg/m^3$, but the weight ratio is lower, around 7%. The main challenge lies in minimizing hydrogen diffusion. To reduce the tank's mass, polymers (type IV) with the best weight ratio are used. However, their permeability is higher than that of steel, resulting in increased hydrogen loss over time.

The volume of hydrogen diffusing through the tank (V_{loss}) can be estimated using the following equation:

$$V_{\text{loss}} = \frac{\mathcal{P} \cdot A \cdot t \cdot \Delta P}{l} \tag{1}$$

Here, $\mathcal{P}$ represents the hydrogen permeability coefficient, A is the surface area of the cylindrical tank, t denotes the duration, ΔP is the pressure inside the tank, and l refers to the liner thickness.

By incorporating an additional 1cm Mylar liner thickness inside the tank, the loss during travel can be kept below 10% of the total hydrogen volume. This loss can be compensated by additional hydrogen. Even with this additional mass, the type IV vessel still has a better mass ratio than a stainless steel vessel.

3.3 Metal hydride

In 2019, the Fraunhofer Institute for Manufacturing Technology and Advanced Materials IFAM released a white paper on hydrogen storage using magnesium hydride MgH_2 [11]. The reaction between magnesium hydride and water can produce hydrogen and magnesium hydroxide, as shown below:

$$\mathrm{MgH_2} + 2\mathrm{H_2O} \longrightarrow 2\mathrm{H_2} + \mathrm{Mg(OH)_2}$$

This solution is highly attractive since hydrogen can be stored for extended periods without any loss (over 5 years), and it is very stable. Furthermore, the mass efficiency is interesting, with 10 kg of Powerpaste releasing 1 kg of hydrogen. However, to produce the required 33 kg of hydrogen, approximately 297 kg of water is needed. It is important to note that Powerpaste is still under development, so relying solely on this storage system is not recommended. Small-scale production of Powerpaste is scheduled for 2023. However, no information is currently available regarding its behavior under radiation, a critical consideration for long space journeys. The total mass of this solution, including the entire supply system, would be around 700 kg.

3.4 Hydrogen storage summary

Among the various options for hydrogen storage, the most promising one is the use of metal hydrides, such as Powerpaste. This solution offers long-term storage capabilities without any hydrogen loss, but it requires the transportation of water for the reaction. However, uncertainties remain regarding its capabilities. With the energy transition, the development of hydrogen storage means should be monitored for the future.

The second best option is compressed hydrogen storage. A type IV tank made of polymers provides a good option due to its reduced mass compared to steel tanks. To ensure low permeability, an additional Mylar layer must be incorporated. For instance, a tank designed to store 40 kg of hydrogen at 70 MPa occupies a volume of $1.10m^3$ and weighs 650 kg. Temperature control is not expected to pose significant challenges as it can be regulated.

Regarding the LH2 option, it carries inherent risks due to its sensitivity to even slight temperature changes, leading to potential failures caused by boil-off. The extreme variations in conditions during EDL phases make this option dangerous. A detailed specification comparison of the different storage options is provided in table 4.

Table 4: H_2 storage summary

Specification	Hydride	cH2	LH2
Mass [kg]	700	690	240
Volume [m^3]	0.8	1.1	0.5
Stability	very high	medium	very low
Energy consumption	low	very low	high
Complexity	medium	low	high
Flow rate	medium	high	low

4. Attachment solutions

In this section, we will try to deal with all the possible solutions for attaching the gondola to the balloon. Obviously, there are other solutions than those presented here. The ones we have chosen seem to be the most suitable and obvious after discussions and readings about projects similar to ours. This pre-study gives an overall idea of the attachment system, but does not yet give the details of the design, which will be dealt with later.

4.1 Central skirt

When we think of a balloon flying with the help of Archimedes' thrust, we think directly of a hot air balloon. Most of them have what we call a skirt. It allows to protect the flame of the burner from the wind. It is often also this part to which the gondola is directly attached. Its shape, slightly tangent to the balloon, allows to distribute the stresses well while avoiding a too important deformation of the latter. This type of shape is also used for airship gondolas.

4.2 Cables tangent to the balloon

A second system for attaching the gondola to a balloon is to pull a series of cables positioned between each tendon of the envelope. This method is frequently used on hot-air balloons and airships. The purpose of these cables is to be relatively far from the gondola so that they are tangent to the balloon, which allows to better distribute the constraints and to avoid pitching problems.

4.3 Central attachment

When we want to attach an object to another, the simplest and most obvious solution at first sight seems to be a rope. Indeed, when we don't have any constraint of load distribution, pitch (pendulum effect) or rigidity, it is certainly the cheapest and easiest way to implement. In our balloon case, it would theoretically be possible to think in the same way. This is what NASA has done with its SuperTIGER balloon [12]. The attachment of the gondola is done directly from the end of the balloon's axis of revolution. This choice allows to have the lowest possible mass. Nevertheless, it is necessary to keep in mind that the conditions of flight in their case, at very high altitude, were optimal. The climatic

disturbances such as the wind are non-existent and thus the pitching of the gondola and the balloon are not a problem. Unfortunately, we cannot make the same considerations on Mars.

This type of attachment concentrates all the load in one point. It is therefore necessary to know if this can cause a significant deformation of the balloon and therefore an increase in the internal pressure of the balloon. For this purpose, a numerical calculation studying the case in a simplified way was carried out. It is realized that the pressure variation is of the order of 0.0014%. This shows us that it can be neglected and that the deformation caused by a central attachment is not problematic.

4.4 Summary, comparison table and choice

Now that we have described all the different solutions, we are able to present a comparative table evaluating each of them. The criteria and weighting factors were determined according to their importance for this particular project and assignment.

		Score out of 10		
Criteria	weighting factor	Central skirt	Central attach	cables tangent to the balloon
Ease of design	1	5	10	7
Ease of manufacturing	1	4	10	6
Control and distribution of stress	2	10	3	4
Risk of vibration	2	10	1	3
Pitch and instability of the gondola	3	10	1	8
Mass of the system	4	7	10	5
Total		8,23	5,46	5,46

Figure 7: Comparison score for Attachment

The average final score naturally shows us that the central skirt solution is the most optimal in our case. The rest of the balloon design will thus be done using this attachment system. Given the likely size of the gondola compared to the balloon, we imagine that the skirt's diameter would be between 2 and 4m. What's more, the skirt would be added to the balloon (by gluing or weaving). Its sole function is to transmit forces and hold the basket. It is not intended to ensure the impermeability of the hydrogen.

5. Choice of envelope materials

Let us recall that for the design of a hydrogen balloon, it is necessary to have a layer that is impermeable to hydrogen (or at least as much as possible). Unfortunately, the materials that can fulfil this function often have poor mechanical, thermal, erosion and UV resistance properties. It is therefore necessary to add a second layer that fulfils these other functions. There are two types of solutions to hold these two layers together. In the first case, we consider two separate layers of different materials that are simply in contact. In the second case, we consider two layers of different materials joined by an assembly method (gluing, riveting). It has been clearly demonstrated in previous works [9] [13] that mylar is the best solution to conserve hydrogen. It is today the most used material to fulfil this function. It is moreover the one that has been chosen for the majority of the existing hydrogen balloons to date, including for the balloon developed by NASA [6]. So mylar was an inevitable choice, we still need to find a material for the second layer.

5.1 Two seperated materials

As mentioned above, the two materials are not joined and therefore not bonded, which means that they can deform freely. It is very important to take this into consideration because it implies that the materials can have completely different mechanical and thermal properties, as the deformation of one does not influence the other. Knowing this, we can then focus on the desired criteria of each material without considering the choice of the other.

After making a study taking into account that the most important criterion is clearly the ratio yield strength / density, the most suitable materials are: Dyneema, Vectran and Zylon (PBO fibers, Kevlar).

Thanks to a stress pre-study based on the data of [9], we realized that for high strength fibers (from about 1000 MPa), the thinnest existing layer is sufficient. This means that even with the thinnest layer that can be manufactured (around 26 μm for dyneema, for example), the yield strength is never reached. Logically, density becomes the predominant criterion. The resistance to UV radiation is also an important point since this layer will be directly exposed to radiation. In this sense, dyneema seems to be the most optimal solution if we want to have the smallest and lightest balloon possible. Moreover, this fiber is the one that best preserves its properties when reaching the lowest mission temperatures (about 180 K), unlike the other two which may deteriorate slightly (an effect that is difficult to estimate, it would be necessary to measure it in order to really know what its impact is).

5.2 Two joined materials

Let us now consider the second case of material choice, namely when the two layers are joined. This implies that the two materials must deform in the same way in the direction of the joint. Thus, significantly different coefficients of thermal expansion and Young's moduli could cause significant stresses in case of pronounced temperature differences. In addition to the solutions proposed in the previous chapter (dyneema being the best choice), we will propose a material whose thermal and mechanical properties are closer to mylar in order to have an alternative if the stresses due to temperature differences were to be too important with dyneema. After a detailed search using the Granta Edupack software, we found only one alternative that would allow us to reduce the thermal stresses while keeping the other required properties (UV resistance, low temperature resistance, ...). It would be BMI/HS carbon fiber. This type of carbon fiber is prepreged with Bismaleimide (BMI) Resin. Even if this fiber is much denser than dyneema, it is still interesting thanks to its thermal expansion coefficient being closer to that of mylar.

6. Impermeable structural solutions

In this section, we will deal with all the possible solutions to link the impermeable layer to the fiber layer. As for the attachment system, there are other solutions than those presented here. The ones we have chosen seem to be the most suitable and obvious after discussions and readings about projects similar to ours. This pre-study gives an overall idea of the assembly system between the layers, but does not yet give the details of the design, which will be dealt with later in the project.

6.1 Hydrogen Balloon

Some zeppelins do not have directly an external envelope which contains the carrier gas, but have an inner balloon fulfilling this function. This allows the height to be metered directly by filling or emptying the balloon. This method is possible when it is not necessary for the filling/deflation action to be reversible. That is, when the airship reaches a maximum height and then gradually descends without ever having to climb back up. Otherwise, it would be necessary to refill the balloon with gas, which becomes costly and useless when you consider that you can simply add balloons of ambient air in order to make the airship heavier or not. It is moreover the solution that we had chosen previously in this project [13]. We then avoid weighing down the gondola unnecessarily by keeping hydrogen tanks but we simply fill balloons with ambient Martian air with the help of a pump. Nevertheless, even if we will not use the hydrogen balloon system in this way and we will keep our hydrogen mass constant during the flight, this method has some advantages in terms of structure and stress distribution. Indeed, it is interesting to have a balloon of the same size as the outer layer simply establishing a mechanical contact with it instead of joining the layers by any assembly method.

A problem with having a hydrogen balloon is that the contact areas between the balloon and the upper layer may decrease depending on the difference in elasticity or thermal expansion between the materials. Therefore, it is necessary to quantify this possible loss of contact. A numerical calculation made from the data of [9] allowed us to deduce a maximum difference of 1.57% between the two layers for the radius and about 4.6% for the volume.

6.2 Bonding

The second solution we will present here is bonding. It is certainly the most intuitive, but it is not the easiest to implement. This method, which is extremely well known and used for all types of applications, varies enormously depending on the type of material, the type of adhesive, the type of surface, the surrounding environment, etc. There are therefore many parameters to take into account and its manufacture requires particular rigor, precision and method. The quality of the bonding can vary considerably from one case to another. Nevertheless, it remains a safe way to establish a constant contact between two layers (on the contraey, this does not mean that the mechanical properties of the assembly will be known nor mastered).

6.3 Gas-tight riveting

Another well-known and frequently used joining method is riveting. Although used primarily for rigid materials, such as steel joints, it is also used for flexible structures. For example, we often see rivets on fabrics to join the different layers (jeans or bags in particular). In the case of our balloon, there is an obvious problem of impermeability. Since on of the two layers' purpose is to retain the hydrogen, it would be preferable not to pierce it if we want to avoid any gas leak. For this reason, it is necessary to perform an impermeable riveting. Such rivets exist today, however with some uncertainty as to the reliability of the seal depending on the quality of manufacture and assembly.

6.4 Summary and choice

Firstly, we can easily eliminate the riveting solution because it simply carries too many risks regarding the hydrogen-sealing in view of the thinness of the layers. Furthermore, it would distribute the stress unevenly and unnecessarily increase the mass of the system. We would then have to choose between bonding and the hydrogen balloon. At this point, it is too difficult to know which solution would be ideal for the balloon. Even though the hydrogen balloon solution has many advantages in terms of convenience and reliability of design, it is necessary to size both types of balloons in order to know already if the solution is feasible but also which of the two gives the lowest total mass. Thus, the optimum solution will be chosen after carrying out both studies.

7. Design of the hydrogen balloon

In order to know which solution is preferable for the envelope structure, it is necessary to dimension both types of balloons, i.e. with bound and unbound layers. This will give us an idea of the feasibility as well as the size of the balloon if it is feasible. In this section, we will then start with the solution presenting a hydrogen balloon, that is with 2 separate layers.

7.1 Calculation of the maximal pressure

The hydrogen balloon is dimensioned by taking the worst case of internal pressure. To do this, we will first determine the maximum overpressure due to the Martian air balloon. It is possible to find a pressure ratio between the lowest and the highest pressure due to this effect. Using Newton second law and the law of ideal gases, the ratio is:

$$RatioP = \frac{1}{1 - \frac{\rho_{atm,max} - \rho_{atm,min}}{\rho_{atm,max}}} \tag{2}$$

Then, we will calculate the minimum pressure necessary inside the balloon. There are 3 cases where a minimum pressure is required to prevent the balloon from collapsing or changing shape:

- The pressure due to solar cells (if the cells are on the balloon)
- The pressure due to the total weight (normal force)
- The wind pressure

Each of these 3 cases exerts a pressure on the balloon that must be countered by the internal pressure to ensure that the balloon keeps its shape. The goal is then to know which of these 3 cases requires the highest pressure. This will allow us to know the minimum pressure inside the balloon. The resolution of the 3 cases shows us very clearly that the highest pressure is due to the solar panels. This will finally lead us to the calculation of the maximum pressure by taking the overpressure due to the Martian air balloon and adding the effects of temperature increase. So we multiply the minimal pressure by the ratioP calculated with relation 2 and then we apply the law of perfect gases in order to take into account the temperature effects as follows: Considering the volume and the mass as constant, we have:

$$P_2 = \frac{T_{max}}{T_{min}} P_1 \tag{3}$$

The value of the maximum pressure thus depends on the initial pressure and the temperature difference given by the thermal model. An interesting figure that we can bring out is the ratio of pressure between the minimum one that we would have at the highest altitude and the lowest temperature and the maximum one at the lowest altitude and the highest temperature. With the thermal model of [13] and the data of [9], this ratio would be 2,02.

7.2 Dimensions of the balloon

Knowing the critical cases of internal pressure, we can now dimension the mylar layer. It has been shown through a pre-dimensioning calculation that the minimum thickness of the dyneema layer (26 μm) is more than sufficient in terms of mechanical strength when the layers are separated. This parameter can therefore be considered as fixed. Then, knowing that the pressure calculation depends on the size of the balloon, itself depending on the thickness of the mylar layer, it was necessary to realize a calculation code working on a principle of incrementing the thickness until we are below a certain value of stress. Set at 40 MPa for the mylar (taking a safety margin of about 20% with respect to the yield strength), we obtain the following results:

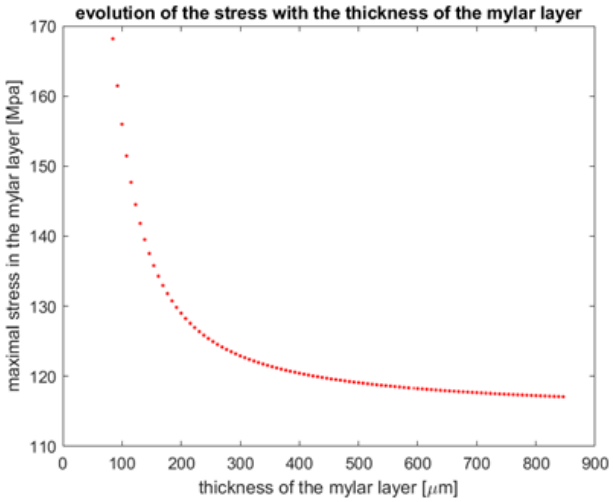

Figure 8: Evolution of stress for hydrogen balloon

Unfortunately, it can be seen from figure 8 (calculated for a gondola mass of 350 kg) that the increase of the layer thickness has an asymptotic tendency and therefore cannot find a solution for a stress below 40 MPa. This is due to the fact that by increasing the thickness of the layer, even if the force is distributed better, it increases because the size of the balloon also increases. It is therefore impossible to size a mylar hydrogen balloon with a gondola mass of 350 kg and an internal Martian air balloon. It is important to note that the latter increases the internal pressure of the balloon considerably. By eliminating this effect, thus by placing it outside for example, one reaches the limit of constraint fixed when the layer of mylar is 130 μm which gives a balloon of approximately 90m of diameter. This remains consistent.

8. Design of the Balloon with bonded layers

Contrary to the sizing we have just done for the 2 seperated layers, for the 2 bonded layers, it is necessary to take into account the stresses due to thermal expansion effects in addition to the mechanical stresses due to the internal pressure. Once we know these, we can then dimension the balloon by presenting two material solutions, as mentioned in section 5. First, we will see the dimensioning with a dyneema / mylar assembly and then in a second time with a BMI/HS carbon / mylar assembly.

8.1 Evaluation of thermal stresses

If two layers are joined, they must deform in the same way. This can lead to significant additional stresses during a temperature change if the thermal expansion coefficients of the two materials in question are significantly different. Indeed, the layer that expands less will tend to "hold" the other one, which causes some stress. It is possible to evaluate the impact of these stresses quite quickly by using Hooke's law. In order to facilitate the solution of the problem we will assume that the ball is spherical and not elliptical. This simplification is largely acceptable because the difference between the two radii of the ellipse is small. The second assumption that we make is about the boundary condition for the deformation at the interface of the two layers. Since the layers are extremely thin compared to the size of the balloon, it is possible to apply the thin film theory and thus consider that the whole layer deforms in the same way and not only the face in contact.

8.2 Evaluation of the stresses due to pressure

The calculation made for the evaluation of the maximum pressure difference between the inside and the outside of the balloon in point 5 can also be used in the case of joined layers. The calculations of pressure due to wind and solar panels would not change at all. On the other hand, there would be a difference between the two cases for the calculation of the pressure due to the total weight of the hydrogen balloon (in the case of joined layers, it would only be the pressure due to the buoyancy effect). But since the pressure due to the solar panels is much more important than the other two, it is possible to use the same calculation as before.

8.3 Evaluation of the maximum stress and dimensioning of the balloon

Note that the two types of stresses must not be added together in order to have the maximum stress because the mylar compresses to resist the expansion while it relaxes when there is a pressure difference between the inside and outside of the balloon. Thus, we would add a negative stress to a positive one. It is then necessary to observe which stress among the two is the highest, which gives the most critical case.

8.3.1 Dimensioning with dyneema

When dyneema and mylar are joined, the difference in stiffness between the two materials is such that the pressure stress becomes sufficiently low regardless of the thickness of the layers to be well below the set 40 MPa. On the other hand, the large difference between the thermal coefficient values causes significant thermal stresses in the mylar layer. The evaluation of the stress as a function of the thickness of the mylar layer was performed using a numerical solver. Taking again the temperature differences found in reference [13], we would then have a maximum stress around 36,5 MPa for the thinnest mylar layers (3 μm). It can be seen that the value is extremely close to the limit value we had set. At this point, it is interesting to observe if the increase in the thickness of the mylar layer has a significant influence on the value of the maximum stress and therefore if it is possible to design with a greater safety margin.

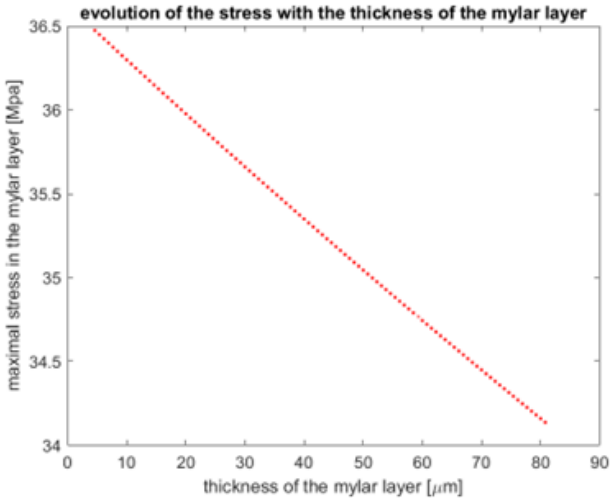

Figure 9: Evolution of stress for dyneema bonded layer

On the figure 9 we can observe the evolution of the stress according to the thickness of the mylar layer. We can easily see that the increase in thickness has unfortunately very little influence and does not allow to obtain a better safety margin on the dimensioning. For a thickness of 3 μm, the balloon would have an average diameter of 43 meters.

8.3.2 Dimensioning with BMI/HS Carbon

In this case, it can be seen that it is the mechanical stress that poses a problem and not the thermal stress, contrary to what was observed for dyneema. Unfortunately, the mechanical stress tends to increase when the mylar layer is thickened (figure 10).

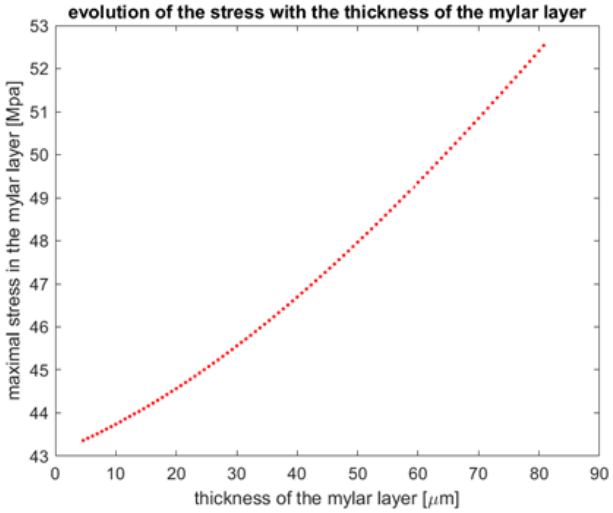

Figure 10: Evolution of stress for dyneema bonded layer

If we recall the sizing done previously, we will then remember that the maximum stresses for a pumpkin shape are in the tendons. These are indeed the stresses that are shown in Figure 6. The value would be 43,36 MPa when the mylar thickness is 3 μm. With this same dimension, the maximum stress would be 34,69 MPa in the rest of the structure. There is also a new issue: the stress in the fiber. Previously, dyneema was not a problem with the thinnest fiber layer available, 25 g/m^2. However, the elastic limit of carbon (507 MPa) is much lower and with such a thickness, the stress in the tendons would exceed this limit (658 MPa). Moreover, the stress in the mylar exceeds the limit value of 40 MPa that we had set. It would therefore be necessary to reinforce the tendons. With a mass per unit area of 40 g/m^2 of carbon in the tendons, the stress would be 441 MPa for the carbon and 29,32 MPa for the mylar, i.e. below the limits set. By dimensioning the balloon in this way, it would then reach an average diameter of 44 meters. In conclusion, as for dyneema, it is possible to size the balloon with a BMI/HS Carbon layer but with relatively small safety margins.

9. Choice of the impermeable structural solution

The studies carried out in previous points clearly show us that it is preferable to opt for the solution of glued layers rather than that of the hydrogen balloon. Indeed, we found that even if we remove the overpressure effect of the Martian air balloon, the balloon would have to be of an extremely large diameter (90 m) if we wanted to be below the limit values of stress. Concerning the solution of glued layers, we presented two alternatives of materials. In the end, both are equal and can be considered. The choice would certainly depend on the manufacturing process and its reliability. The ease of bonding, weaving and assembly would be the predominant argument. Knowing that in the case of dyneema, the maximum stress comes from the effects of thermal expansion, let's recall that we had found that thermal stresses did not depend on the radius of curvature. It would then be possible to design a perfectly smooth balloon, without tendons and which would not be pumpkin-shaped.

10. Conclusion

This study has explored various options concerning the deployment method, the hydrogen storage, the design of the envelope and the attachment system. The aim was to assess the different solutions, determine the best solution and continue the feasibility study for this Martian airship.

Four concepts of deployment were developed and analyzed. The deployment of an airship with a diameter of 43m is a challenge. The method of ground deployment is the best out of the four. Other concepts have shown their limitations. However, the ground solution comes with technical difficulties for unfolding. The airship's large envelope size and the need for safety require innovative and reliable techniques. One method considered is to use a supporting cone to facilitate the controlled release and deployment of the envelope and protect the system against external hazards. The techniques for deploying the envelope is the main obstacle to the feasibility of this project and further work has to be done.

For hydrogen storage, metal hydride such as Powerpaste as a hydrogen storage medium emerges as a privileged option. Metal hydride offers the advantage of long-term hydrogen storage capability, allowing for the safe and efficient storage of hydrogen for extended durations. Compressed hydrogen offers an alternative option.

Concerning the attachment solutions, we have easily shown that the central skirt solution had the most advantages and should be considered for the continuation of the project. Then, the parallel study of the choice of materials and the structure and assembly system showed us that it was preferable to join the layers by gluing. At this stage, we recommend two solutions, namely a dyneema / mylar assembly or a BMI/HS carbon / mylar assembly. Both can be considered and the determining criterion will be the ease and reliability of design. The realization of a complete numerical solver was made and allows to give the dimensions of a balloon with these two assemblies. It would be necessary however to think of a light reinforcement of the zone close to the central skirt for the solution with the carbon fiber. For the continuation of the project, it could thus be envisaged to carry out a 3D model and a deepening of the solution of attachment starting from materials and dimensions given in this report.

11. Acknowledgement

We would like to thank the previous groups who worked on this project: Romeo Tonasso, Florentin Fellay, Biselx Michael and Vincent Roggli, for their time. WoMars association represented by Laurène Delsupexhe and Alice Barthe for their feedback and help. The Mars Society Switzerland: Claude Nicollier and Pierre Brisson for their assistance and supervision throughout the semester. For this work, we have conducted interviews to acquire more information on specific domains. We thank Stratobus, Chaix Rodolphe and Combet Yannick for their time and important advice on flexible structure in a high atmosphere. We thank the Mars Society Deutschland and Klaus Bayler for their time and help with the feasibility of the mission.

References

[1] R. Tonasso, L. Delsupexhe, and A. Barthe, "Can an airship explore mars?" *GLEX-2021*, x62378, Jun. 2021.

[2] M. W. Biselx, F. Fellay, and V. J. Roggli, "Envelope, propulsion and navigation for a martian exploration airship," *IAC-22-A3.3B*, x69999, 2022.

[3] A. Nelessen, C. Sackier, I. Clark, *et al.*, "Mars 2020 entry, descent, and landing system overview," in *2019 IEEE Aerospace Conference*, 2019, pp. 1–20. DOI: 10.1109/AERO.2019.8742167.

[4] H. S. Griebel, "Methoden der ballonentfaltung auf dem mars," in *PDM TUM*, 2022, pp. 1–123. DOI: RT-DA03/01.

[5] J. A. D. Corso, W. E. Bruce, S. J. Hughes, *et al.*, "Flexible Thermal Protection System Development For Hypersonic Inflatable Aerodynamic Decelerators," en, in *9th International Planetary Probe Workshop, Conference and Seminar*, 2012.

[6] J. Hall, M. Pauken, V. Kerzhanovich, *et al.*, "Mars Balloon Flight Test Results," en, in *AIAA Balloon Systems Conference*, Seattle, Washington: American Institute of Aeronautics and Astronautics, May 2009, ISBN: 978-1-62410-136-6. DOI: 10.2514/6.2009-2809. [Online]. Available: https://arc.aiaa.org/doi/10.2514/6.2009-2809 (visited on 10/10/2022).

[7] J. T. Bruton, "Packing Sheet Materials Into Cylinders and Prisms Using Origami-based Approaches," en, in *Brigham Young University ScholarsArchive*, BYU.

[8] N. Atkinson, "Nasa funds development of mars balloon," *Universe Today*, Feb. 2009, Accessed on May 7, 2023. [Online]. Available: https://www.universetoday.com/25964/nasa-funds-development-of-mars-balloon/.

[9] T. Romeo, "Martian airship for geological exploration," en, *Semester Project Report*, 2020.

[10] H. Barthelemy, M. Weber, and F. Barbier, "Hydrogen storage: Recent improvements and industrial perspectives," en, *International Journal of Hydrogen Energy*, vol. 42, no. 11, pp. 7254–7262, Mar. 2017, ISSN: 03603199. DOI: 10.1016/j.ijhydene.2016.03.178. [Online]. Available: https://linkinghub.elsevier.com/retrieve/pii/S0360319916305559 (visited on 10/10/2022).

[11] R. Lars, "Powerpaste For Off-Grid Power Supply Whitepaper," en, in *Fraunhofer Institute for Manufacturing Technology and Advanced Materials IFAM, Branch Lab Dresden*, 2019.

[12] R. Garner, "Nasa's supertiger balloon flies again to study heavy cosmic particles," Dec. 2017. [Online]. Available: https://www.nasa.gov/feature/goddard/2017/nasas-supertiger-balloon-flies-again-to-study-heavy-cosmic-particles.

[13] R. Vincent, "Superpressure balloon for mars exploration balloon modeling, materials, and shape analysis," en, *Semester Project Report*, 2021.